Applied Surface Science 464 (2019) 153–161

Contents lists available at ScienceDirect

Applied Surface Science

journal homepage: www.elsevier.com/locate/apsusc

Full Length Article

Adsorption of the NH_3, NO, NO_2, CO_2, and CO gas molecules on blue phosphorene: A first-principles study

F. Safari[a], M. Moradinasab[b], M. Fathipour[b,*], H. Kosina[c]

[a] Department of Electrical Engineering, Arak Branch, Islamic Azad University, Arak, Iran
[b] Device Simulation and Modeling Laboratory, School of Electrical and Computer Engineering, Faculty of Engineering, University of Tehran, Tehran, Iran
[c] Institute for Microelectronics, TU Wien, Wien, Austria

ARTICLE INFO

Keywords:
Blue phosphorene
Gas sensor
First-principles
NEGF

ABSTRACT

We report on a first-principles study of the electronic and transport properties of pristine, B-, C-, N-, O-doped blue phosphorene (BlueP) with the adsorption of gas molecules NH_3, NO, NO_2, CO, and CO_2. The adsorption distances, adsorption energies, charge transfer, density of states (DOS), and transmission spectra of these gas molecules on molecules on doped as well as undoped BlueP is systematically investigated in this work. Our calculations show that the adsorption energy of NO and NO_2 on pristine BlueP is the largest among the considered gas molecules, suggesting that pristine BlueP is more sensitive to these two gases. The results indicate that the pristine BlueP exhibits a weak sensitivity to NH_3 and CO molecules, while B-doped BlueP strongly adsorbs NH_3 and CO by way of strong chemical bonds. C-doped BlueP can enhance the sensitivity to NH_3 gas molecules. The current-voltage (I-V) characteristics of the sensors are calculated using non-equilibrium the Green's function (NEGF) formalism. Theses sensors show characteristic responses along both the zigzag and the armchair directions depending on the type of the gas molecules.

1. Introduction

Sensing toxic gas molecules is critical in environmental pollution monitoring, control of chemical processes, and agricultural and medical applications [1]. Two-dimensional (2D) materials offer great potential applications for gas sensing due to their unique properties and large surface-to-volume ratio [2]. Phosphorene, a new 2D material, has recently been exfoliated by mechanical cleavage of black phosphorus, the most stable allotrope of the element phosphorus in ambient condition [3]. The high hole carrier mobility and direct band gap of phosphorene promise new applications in electronics and optoelectronics [4–11]. First-principles calculations indicate that adsorption of gas molecules such as NO_2, NO, NH_3 and SO_2 induces appreciable variations to the electronic and transport properties of phosphorene [12–18], revealing the promising sensing capability of this 2D material. Blue phosphorus, a new allotrope of phosphorus, was first predicted by Zhu et al. in 2014 [19], and a molecular-beam epitaxial growth of its single layer on Au (1 1 1) has been reported by Zhang et al. in 2016 [20]. It is an indirect gap semiconductor with the band gap of about 2 eV [19]. Theoretical studies have been carried out to investigate the interactions of blue phosphorene (BlueP) with different molecules [21–23], however, the effect of such molecules on transport properties of BlueP is still lacking.

In this work, we investigate sensing performance of pristine, B-, C-, N-, and O- doped BlueP exposed to five gas molecules (NH_3, NO, NO_2, CO, and CO_2). Our first-principles calculations reveal that gases induce recognizable states in the density of states (DOS). The current-voltage (I-V) characteristics of the BlueP and doped systems are calculated before and after gas absorption using a non-equilibrium Green's function (NEGF) formalism. The results indicate that the adsorption of various gas molecules induce remarkable variations in I-V characteristics which renders BlueP and doped systems as a promising candidate for novel gas sensors.

2. Methods

Structural relaxation and electronic calculations are performed by first-principles calculations based on the density functional theory (DFT) as implemented in the SIESTA program package [24]. The generalized gradient approximation (GGA) with the Perdew-Burke-Ernzerhof (PBE) exchange–correlation functional is employed [25]. To describe the Van der Waals interactions between substrates and gas molecules and to achieve accurate results, the DFT-D2 method of Grimme is implemented [26]. The double zeta polarization (DZP) basis set is used to optimize all the systems. During the optimization, all

* Corresponding author.
E-mail address: mfathi@ut.ac.ir (M. Fathipour).

https://doi.org/10.1016/j.apsusc.2018.09.048
Received 13 April 2018; Received in revised form 8 August 2018; Accepted 5 September 2018
Available online 06 September 2018
0169-4332/

atoms in the unit cell are relaxed until the residual force on each atom is smaller than 0.01 eV/Å. The mesh cutoff energy is chosen to 150 Ry. The 3 × 3 rectangular supercell with 36 atoms is used to simulate the pristine BlueP. A vacuum region of 15 Å is added to avoid interaction between the neighboring layers. The mesh for the geometry optimization is set to 3 × 3 × 1 and for the electronic structure calculations to 9 × 9 × 1.

Since NO and NO_2 molecules are paramagnetic, spin polarization is considered for the calculations. To characterize the interaction strength between the molecule and the studied structure, the adsorption energy (E_{ads}) is defined as the energy of the fully relaxed pristine or doped BlueP with a gas molecule adsorbed ($E_{BlueP+gas}$) minus the energy of the isolated pristine or doped BlueP (E_{BlueP}) and an isolated gas molecule (E_{gas}), $E_{ads} = E_{BlueP+gas} - E_{BlueP} - E_{gas}$ [12]. The electronic transport properties are calculated with the TRANSIESTA package based on the NEGF method [27]. The current through the contact region is obtained by the Landauer–Büttiker formula [28].

3. Results and discussions

After substituting B, C, N, and O dopants in pristine BlueP, all the systems are fully relaxed. The results are well consistent with those in previous reports [29,30]. To explore the relative stability of the doped systems, the formation energy (E_f) is defined as:

$$E_f = E_{ds} - n \times E_P - \mu_d$$

where E_{ds} is the total energy of doped system, E_P is the energy of a single P atom in the pristine BlueP, n stands for the number of P atoms in the doped system, and μ_d is the chemical potentials of a doping atom, respectively [31]. The formation energies of 0.66, 2.14, 1.02, and −1.10 eV are obtained for B-, C-, N-, and O- doped BlueP systems, respectively. The calculated formation energies indicate that the considered structures are stable.

For each adsorption configuration, the initial distance between a gas molecule and the substrate is chosen as 2.0 Å. The adsorption distance, defined as the shortest atom-to-atom distance between a gas molecule and the substrate, is calculated, see Fig. 1. For the system NO molecule on pristine BlueP, the adsorption distance of 1.78 Å is obtained. The adsorption distances of 2.74 Å, 2.87 Å, 2.51 Å, and 2.43 Å are calculated for NH_3, CO_2, CO, and NO_2, respectively. The smaller adsorption distance indicates a stronger interaction. The adsorption distances of 1.08, 0.98, 0.89, and 0.99 Å are calculated for NH_3, CO, NO, and NO_2 on B-doped BlueP systems, respectively, which are within the sum of covalent atomic radii of B-N (1.57 Å), B-C (1.59 Å), and B-O (1.55 Å) [21,32]. Therefore, chemical bonds form between the B-doped BlueP system and these gas molecules. For the case of the CO_2 gas molecule, no chemical bonds form because the adsorption distance of 1.78 Å is larger than the sum of the corresponding atom covalent radii (1.59 Å).

The adsorption of the NO and NO_2 gas molecules on the C-doped BlueP results in chemisorption and chemical bonds form because the adsorption distances of 0.92 and 1.08 Å are notably smaller than the sum of the corresponding atom covalent radii (1.52 Å). The results for the NH_3, CO, and CO_2 gas molecules indicate the adsorption distances of 1.94, 1.69, and 2.21 Å, respectively. For the systems NH_3, CO, CO_2, and NO_2 on N-doped BlueP, the adsorption distances of 1.92, 2.00, 2.32, and 1.96 Å are obtained, respectively, which are significantly larger than the sum of covalent atomic radii of N-N (1.50 Å), and N-C (1.52 Å). Thus, chemical bonds are not formed in such systems. The nearest distances of NH_3, CO, CO_2, NO, and NO_2 adsorbed on O-doped BlueP are 1.47, 2.01, 2.31, 1.84, and 2.06 Å, respectively, which are remarkably larger than the sum of covalent atomic radii of O-H (1.11 Å), O-C (1.50 Å), and O-N (1.48 Å). Therefore, no chemical bond is expected to form.

According to its definition, the negative adsorption energy implies that the adsorption of gas molecules on BlueP and doped systems is energetically favorable [2]. The obtained adsorption energies are displayed in Fig. 2. As can be seen, E_{ads} is drastically affected by dopants. In comparison with the pristine BlueP system (E_{ads} = −0.131 eV), E_{ads} of B- and C-doped BlueP (−1.414 and −0.164 eV, respectively) increases with adsorption of NH_3. The calculations show low E_{ads} for CO on all doped systems (except for CO gas molecule on B-doped BlueP). Therefore, such doped systems are not suitable candidates for CO gas molecule detection. It can be seen that all the adsorption energies of NO are negative indicating that such systems are energetically suitable candidates for NO gas molecule detection. For NO_2 on C- and B-doped BlueP systems, the adsorption energies become larger than that of pristine BlueP, and a covalent bond is formed between the N and dopants. As it can be seen in Fig. 2, the adsorption energies of N- and O-doped BlueP systems are lower than that of pristine BlueP. To explore the coverage effect, we consider one NO molecule adsorbed on the 2 × 2 and 4 × 4 supercells of BlueP. The interaction between NO molecule and the BlueP is slightly changed with coverage, resulting in similar E_{ads} (Table 1) and bandgap value.

To further investigate the adsorption process, we have calculated the charge transfer between substrates and gas molecules, see Table 2. The positive charge transfer values denote electron transfer from the substrates to gas molecules, while the negative charge transfer values express electron transfer from gas molecules to the substrates [23]. There is a strong correlation between the adsorption energy and the value of charge transfer. The adsorption of NO induces the largest charge transfer (0.208 e) and large adsorption energy (−0.216 eV) among the five considered gas molecules, indicating that the pristine BlueP has the highest sensitivity to NO. Furthermore, the pristine BlueP is sensitive to NO_2 molecules with relatively large charge transfer (0.189 e) and the largest adsorption energy (−0.484 eV). NH_3 and CO_2 exhibit smaller charge transfer (−0.021 and 0.032 e, respectively) and

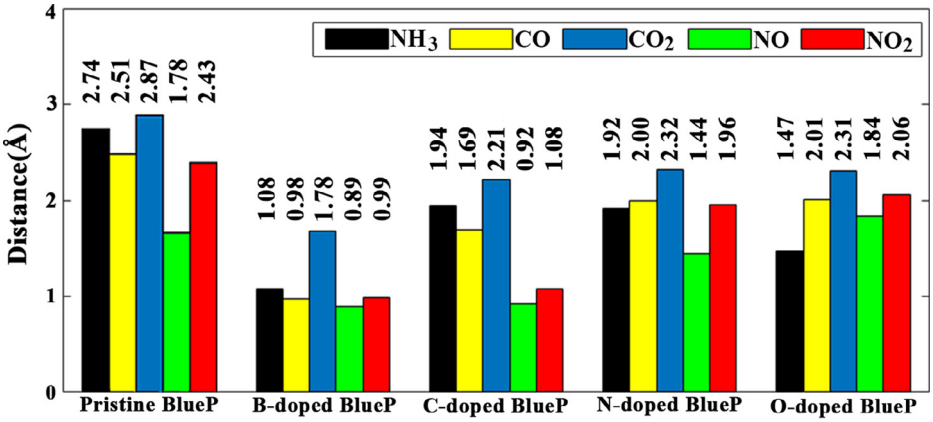

Fig. 1. The absorption distance of gas molecules on BlueP and its doped systems.

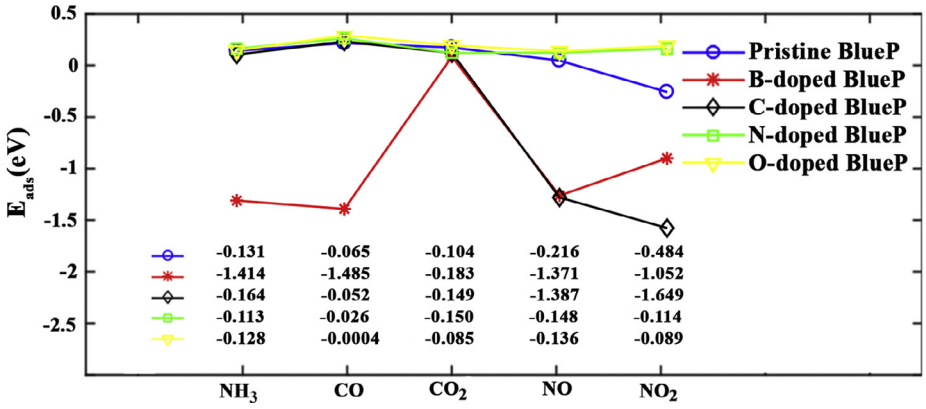

Fig. 2. The adsorption energies for several gas molecules on BlueP and its doped systems.

Table 1
The adsorption energy (E_{ads}) of a single NO molecule adsorbed on BlueP and its doped systems with different supercell sizes.

NO	Supercell		
	2x2	3x3	4x4
	E_{ads} (eV)	E_{ads} (eV)	E_{ads} (eV)
Pristine BlueP	−0.219	−0.216	−0.223
B-doped BlueP	−1.369	−1.371	−1.362
C-doped BlueP	−1.421	−1.387	−1.478
N-doped BlueP	−0.222	−0.148	−0.249
O-doped BlueP	−0.191	−0.136	−0.203

larger adsorption distances in contact with the pristine BlueP. For the case of CO, the charge transfer increases slightly (0.046 e) which is higher than CO_2.

The noticeable charge transfer of 1.074, 0.904, and 0.756 e are obtained from B-doped BlueP substrate when exposed to NO_2, NO, and CO, respectively. The smallest amount of charge (0.026 e) transfers from B-doped BlueP substrate to the CO_2 gas molecule. The charge transfer of 0.135 e is observed for the NH_3 gas molecule. The calculations indicate high charge transfer of 0.521 and 0.383 e from the C-doped BlueP system to the NO_2 and NO gas molecules, respectively. The amount of charge that is transferred from the NH_3 gas molecule to the C-doped BlueP is 0.041 e. Besides, the charge transfer of 0.075 e (−0.051 e) is calculated for NO (NH_3) gas molecule on N-doped BlueP system. The NO gas molecule act as an electron donor and transfers 0.076 e to the O-doped BlueP substrate.

Next, we calculate the density of states (DOS) and the projected DOS to explore the effects of gas adsorption on the electronic properties of pristine BlueP and its doped systems. Fig. 3(a) exhibits the DOS of the pristine BlueP before gas adsorption. For BlueP the DOS are negligibly changed in the presence of CO_2, which is consistent with its small charge transfer and adsorption energy (−0.104 eV), as shown in Fig. 3(b). However, as seen in Fig. 3(c), the adsorbed CO molecule induces defect states in the gap. The adsorption of NH_3 gas molecule induces a defect peak at ∼ −0.75 eV in the DOS (Fig. 3(d)). The adsorption of paramagnetic gas molecules NO and NO_2 on pristine BlueP makes considerable changes in DOS near the Fermi level which results in a magnetic moment of 1 μB, see Table 2. The results are in good agreement with previous studies [13,23].

The DOS of B-doped BlueP system before gas adsorption is presented in Fig. 4(a). Because of the large adsorption distance, the small amount of charge transfer, and the low adsorption energy, no interaction between CO_2 and B-doped BlueP is expected, see Fig. 4(b). The adsorption of CO molecule causes a sharp peak around 1.63 eV in the DOS (Fig. 4(c)). Fig. 4(d) presents the DOS for the NH_3 molecule on B-doped BlueP. It can be seen that the adsorbed NH_3 induces some states at the lower-lying valence bands around −1 eV. By contrast, the adsorption of paramagnetic molecules NO and NO_2 induces a magnetic moment of 1 μB (Table 2). The adsorption of NO molecule gives rise several states of spin up and spin down, respectively, see Fig. 4(e). As shown in Fig. 4(f), there are obvious modifications of the DOS near the Fermi level for the adsorbed NO_2.

We depict the DOS for C-doped BlueP before gas adsorption in Fig. 5(a). The calculations show a magnetic moment of 1 μB for this system, see Table 2. The DOS of C-doped BlueP are insignificantly changed in the presence of CO_2 and CO, which is consistent with their small charge transfer and low E_{ads}, see Fig. 5(b) and (c). The adsorbed NH_3 induces some states over a wide energy range of −1 eV to −2 eV below the Fermi level (Fig. 5(d)). The adsorption of paramagnetic molecules NO and NO_2 modifies DOS near the Fermi level and induce the zero magnetic moment, as demonstrated by Table 2. For the system with adsorbed NO molecule, two defect states appear at energies near −0.6 and 0.6 eV, respectively (Fig. 5(e)). Because of the largest adsorption energy among the all studied systems, NO_2 modifies the DOS of C-doped BlueP, see Fig. 5(f).

The DOS of N-doped BlueP system before gas adsorption is illustrated in Fig. 6(a). Because of the large adsorption distance, the low charge transfer and the low adsorption energy, the adsorbed CO_2 and CO have no significant impact on the DOS of N-doped BlueP, see

Table 2
The charge transfer (Q), band gap (Eg), and Magnetic moment (M) of gas molecules on BlueP and its doped systems.

Gas molecule	Pristine BlueP			B-doped BlueP			C-doped BlueP			N-doped BlueP			O-doped BlueP		
	Q(e)	E_g(eV)	M(μB)	Q(e)	E_g(eV)	M(μB)	Q(e)	Eg(eV)	M(μB)	Q(e)	E_g(eV)	M(μB)	Q(e)	Eg(eV)	M(μB)
None	–	1.98	0	–	1.43	0	–	0.36	1	–	1.26	0	–	0.44	1
NH_3	−0.021	1.78	0	0.135	1.89	0	−0.041	0.32	1	−0.051	1.16	0	−0.064	0.42	1
CO	0.046	1.86	0	0.756	1.93	0	0.064	0.33	1	0.045	1.18	0	0.023	0.36	1
CO_2	0.032	1.98	0	0.026	1.47	0	0.042	0.36	1	0.033	1.29	0	0.026	0.39	1
NO	0.208	0.65	1	0.904	0.75	1	0.383	1.09	0	0.075	0.07	1	−0.076	0	1.6
NO_2	0.189	0.71	1	1.074	0.12	1	0.521	1.77	0	0.111	0.90	1	0.085	0.44	2

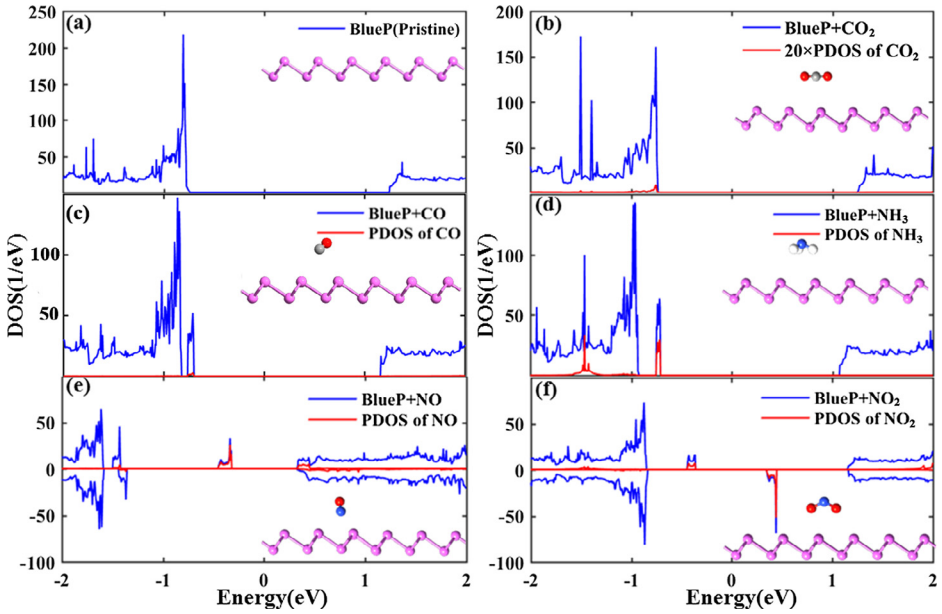

Fig. 3. (a) The density of states (DOS) of pristine BlueP and DOS for molecule-BlueP systems and the projected density of states (PDOS) for (b) CO_2, (c) CO, (d) NH_3, (e) NO, and (f) NO_2, in the adsorption system. The positive and negative values represent spin-up and spin-down states, respectively. Note that the value for the PDOS of the CO_2 is enlarged by a scale factor of 20. The Fermi energy is assumed to be zero. The insets display side view of the fully relaxed structure. The H, C, N, O, P atoms are represented in white, grey, blue, red, and purple colors, respectively. (For interpretation of the references to colour in this figure legend, the reader is referred to the web version of this article.)

Fig. 6(b) and (c). The adsorption of NH_3 induces some states over a wide energy range of −0.5 eV to −2 eV below the Fermi level, as shown in Fig. 6(d). The adsorption of NO and NO_2 molecules on N-doped BlueP causes a magnetic moment of 1 μB, see Table 2. The adsorbed NO gives rise one spin up impurity state near the Fermi level (Fig. 6(e)). However, the adsorption of NO_2 induces one spin down impurity state at ~0.5 eV, see Fig. 6(f). The spin-polarized DOS of O-doped BlueP system before gas adsorption indicates that this system has a magnetic moment of 1 μB (Table 2). The results indicate small charge transfer and low adsorption energy for CO_2, CO and NH3 adsorbent on O-doped BlueP systems, therefor, the DOS remains unaffected near the Fermi level, see Fig. 7(b)–(d). The adsorption of NO molecule induces several distinct spin up and spin down states near the Fermi level, as seen in Fig. 7(e). The results show one spin down impurity for O-doped BlueP exposed to NO_2 gas molecule, as illustrated in Fig. 7(f).

To gain more insight in the gas sensing mechanism, the zero-bias transmission spectra of pristine BlueP and its doped systems are calculated before and after the gas adsorption process, see Fig. 8(a)–(f). The transmission coefficient T(E) of pristine BlueP remains unchanged after adsorption of CO_2 gas molecule. The band gap of pristine BlueP is preserved for CO_2 (1.98 eV) due to the physisorption upon pristine BlueP. This indicates the low sensitivity of pristine BlueP to CO_2 gas molecule. The band gap of BlueP decreases when the substrate is exposed to CO (1.86 eV), NH_3 (1.78 eV), NO_2 (0.71 eV), and NO (0.65 eV). The adsorption of CO and NH_3 on pristine BlueP results in an insignificant change of the T(E), while the adsorption of NO and NO_2 significantly alters the transmission coefficient. The band gap of the doped BlueP is smaller than that of the pristine BlueP, as shown in Figs. 9(a), 10(a), 11(a), and 12(a), respectively.

The transmission coefficient T(E) of B-doped BlueP is negligibly modified in the presence of CO_2 and the band gap of B-doped BlueP (1.43 eV) is increased slightly for CO_2 (1.47 eV) due to insensitivity of B-doped BlueP to CO_2 gas molecule (Fig. 9(b)). The band gap of B-doped BlueP increases upon adsorption of CO (1.93 eV) as well as NH_3 (1.89 eV) while it is reduced upon adsorption of the NO_2 (0.12 eV) and NO (0.75 eV). The adsorption of CO and NH_3 leads to slight change in T(E) of B-doped BlueP, whereas the spin-polarized transmission spectrum is observed for NO and NO_2, as shown in Fig. 9(c)–(f).

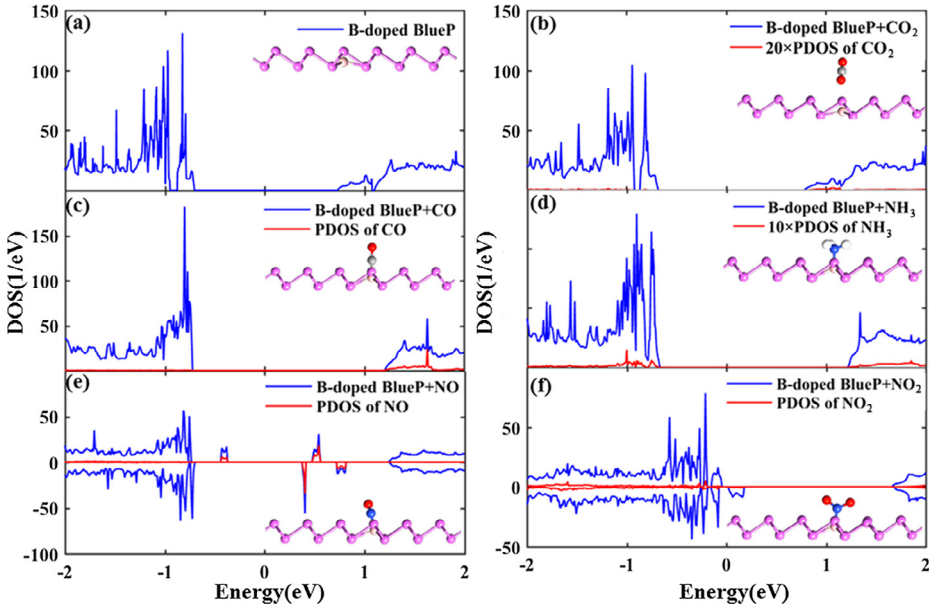

Fig. 4. (a) The density of states (DOS) of B-doped BlueP and DOS for molecule- BlueP systems and the projected density of states (PDOS) for (b) CO_2, (c) CO_2 (d) NH_3, (e) NO, and (f) NO_2 in the adsorption system. The positive and negative values represent spin-up and spin-down states, respectively. Note that the value for the PDOS of the CO_2 and NH_3 arc enlarged by a scale factor of 20 and 10, respectively. The Fermi energy is assumed to be zero. The insets display side view of the fully relaxed structure. The H, B, C, N, O, P atoms are represented in white, pink, grey, blue, red, and purple colors, respectively.(For interpretation of the references to colour in this figure legend, the reader is referred to the web version of this article.)

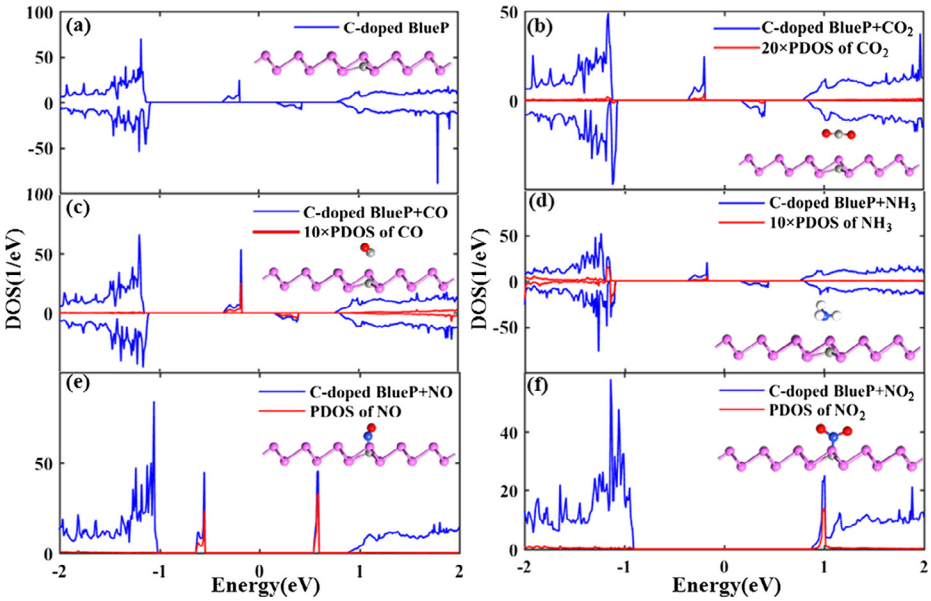

Fig. 5. (a) The density of states (DOS) of C-doped BlueP and DOS for molecule-BlueP systems and the projected density of states (PDOS) for (b) CO_2, (c) CO, (d) NH_3, (e) NO and (f) NO_2, in the adsorption system. The positive and negative values represent spin-up and spin-down states, respectively. Note that the value for the PDOS of the CO_2, CO, and NH_3 are magnified by a scale factor of 20, 10, and 10, respectively. The Fermi energy is assumed to be zero. The insets display side view of the fully relaxed structure. The H, C, N, O, P atoms are represented in white, grey, blue, red, and purple colors, respectively. (For interpretation of the references to colour in this figure legend, the reader is referred to the web version of this article.)

The transmission coefficient T(E) of C-doped BlueP is spin-polarized and the band gap is 0.36 eV as seen from Fig. 10(a). The band gap and T(E) of C-doped BlueP remain unchanged upon adsorption of CO_2, CO, and NH_3 (see Fig. 10(b)–(d)). These results are consistent with the calculated adsorption energies and charge transfers. The band gap of C-doped BlueP is increased for NO_2 (1.77 eV) and NO (1.09 eV) because the transmission spectrum of these molecules do not show any spin-polarization, see Fig. 10(e) and (f). This phenomenon could be attributed to the strong interaction between NO and NO_2 gas molecules and the substrate.

The transmission coefficient T(E) of N-doped BlueP before and after adsorption of CO_2, CO and NH_3 gas molecules shows similar behavior. The band gap of N-doped BlueP (1.26 eV) is increased slightly upon adsorption of CO_2 (1.29 eV) but it is decreased upon adsorption of CO (1.18 eV) and NH_3 (1.16 eV), as illustrated in Fig. 11(a)–(d). The transmission coefficient T(E) of N-doped BlueP is spin-polarized for NO_2 and NO gas molecules (see Fig. 11(e) and (f)) and the band gap of N-doped BlueP is reduced for NO_2 (0.9 eV) and NO (0.07 eV). The band gap and T(E) of O-doped BlueP (0.44 eV) remain unchanged for CO_2, CO, NH_3 and NO_2, as shown in Fig. 12(a)–(e). These results are in agreement with the calculated adsorption energies and charge transfers. The adsorption of NO gives rise to spin gapless transmission, indicating the sensitivity of O-doped BlueP to NO gas molecule (Fig. 12(f)). Note that the real bandgap value may be larger, since DFT-PBE calculations underestimate the size of the bandgap [33].

To further probe the performance of pristine BlueP and its doped systems as a gas sensor, NEGF formalism is employed to calculate the I–V characteristic along the zigzag and armchair directions. As shown in Fig. 13(a) and (b), the currents are zero when the bias is less than 2.0 V, which is attributed to the intrinsic bandgap of pristine BlueP. Fig. 13(a) exhibits the I-V characteristics along the zigzag direction of pristine phosphorene with and without the gas molecule adsorption. Under a bias of 2.4 V, the current passing through the pristine BlueP is about 4.22 μA. However, the current increases to 5.23 μA (10.89 μA) under the same bias when the BlueP is exposed to NO (NO_2) gas molecule. Therefore, the adsorbed gas molecules increase the conductivity as compared with the pristine BlueP. On the contrary, the change in the current induced by NH_3, CO and CO_2 adsorbents is negligibly small in

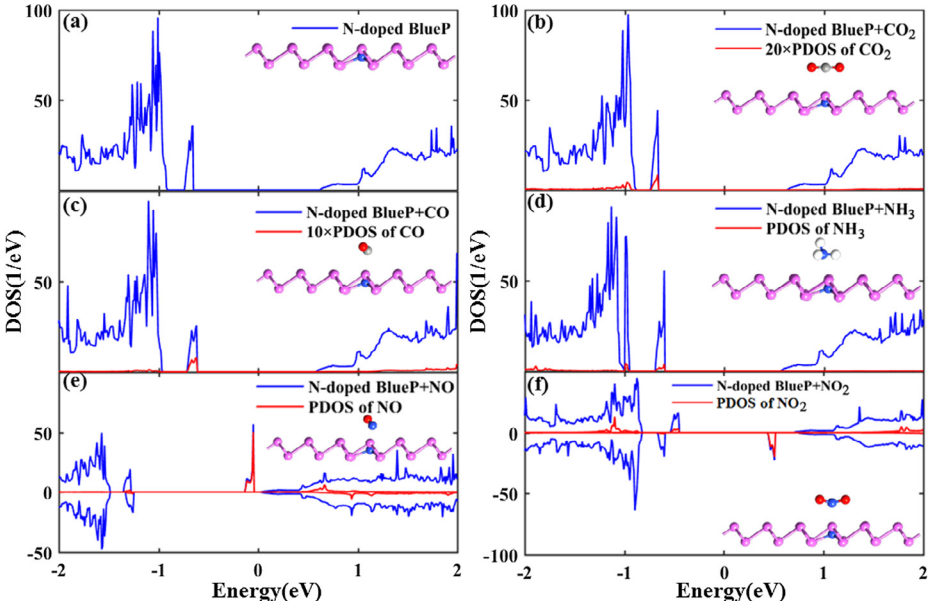

Fig. 6. (a) The density of states (DOS) of N-doped BlueP and DOS for molecule-BlueP systems and the projected density of states (PDOS) for (b) CO_2, (c) CO, (d) NH_3, (e) NO, and (f) NO_2 in the adsorption system. The positive and negative values represent spin-up and spin-down states, respectively. Note that the values for the PDOS of the CO_2, and CO are magnified by a scale factor of 20 and 10, respectively. The Fermi energy is assumed to be zero. The insets display side view of the fully relaxed structure. The H, C, N, O, P atoms are represented in white, grey, blue, red, and purple colors, respectively. (For interpretation of the references to colour in this figure legend, the reader is referred to the web version of this article.)

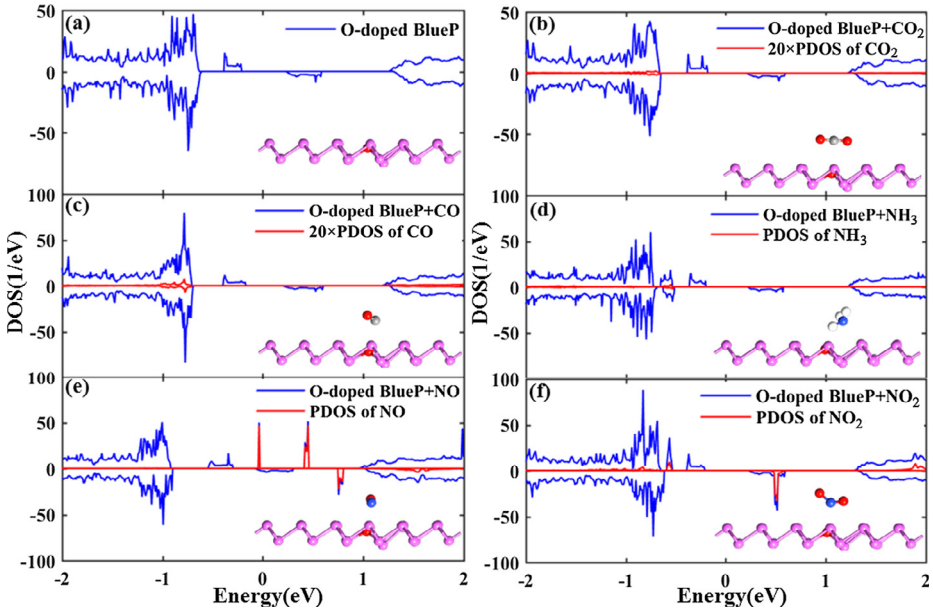

Fig. 7. (a) The density of states (DOS) of O-doped BlueP and DOS for molecule-BlueP systems and the projected density of states (PDOS) for (b) CO_2, (c) CO, (d) NH_3, (e) NO and (f) NO_2 in the adsorption system. The positive and negative values represent spin-up and spin-down states, respectively. Note that the values for the PDOS of the CO_2 and CO are magnified by a scale factor of 20. The Fermi energy is assumed to be zero. The insets display side view of the fully relaxed structure. The H, C, N, O, P atoms are represented in white, grey, blue, red, and purple colors, respectively. (For interpretation of the references to colour in this figure legend, the reader is referred to the web version of this article.)

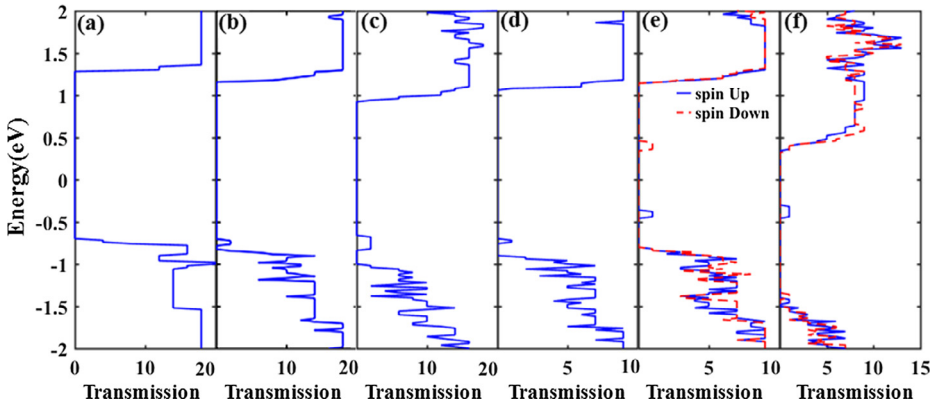

Fig. 8. The zero bias transmission spectrum of (a) pristine BlueP before and after (b) CO_2, (c) CO, (d) NH_3, (e) NO_2, and (f) NO gas molecules adsorption. The Fermi level is set to zero. The blue and red dashed lines represent spin up and spin down states, respectively. (For interpretation of the references to colour in this figure legend, the reader is referred to the web version of this article.)

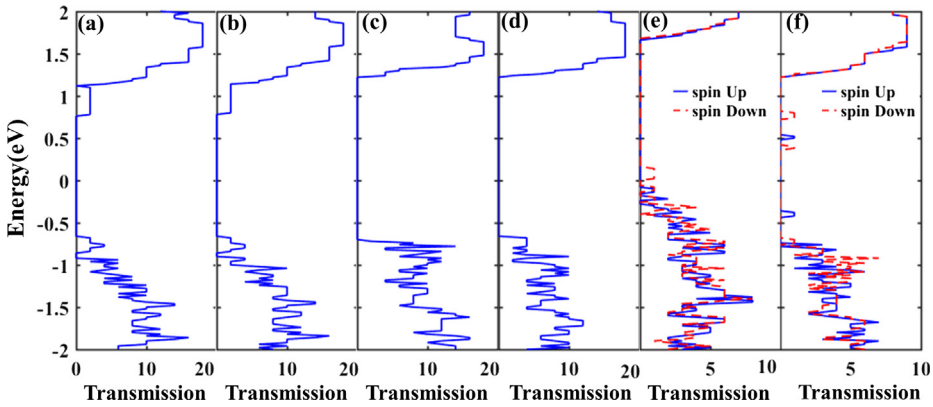

Fig. 9. The zero bias transmission spectrum of (a) B-doped BlueP before and after (b) CO_2, (c) CO, (d) NH_3 (e) NO_2, and (f) NO gas molecules adsorption. The Fermi level is set to zero. The blue and red dashed lines represent spin up and spin down states, respectively. (For interpretation of the references to colour in this figure legend, the reader is referred to the web version of this article.)

the case of zigzag direction, as illustrated in Fig. 13(a). Under the same bias condition, the current passing through BlueP with adsorbed CO_2, CO and NH_3 along the zigzag direction are calculated as 4.75, 4.31, and 4.12 μA, respectively. The I-V curves of pristine BlueP along the armchair direction are displayed in Fig. 13(b). The current along the armchair direction is about 10 orders of magnitude smaller than that for the zigzag direction. The reduction in current indicates the increase in resistance of this material after the adsorption of NH_3, NO, CO and CO_2, which can be measured directly in experiment. Interestingly, the NO_2 adsorption induces a negative resistance along the armchair direction in bias range of 2.6–2.8 V, which is in good agreement with the previous work for black phosphorene [15].

The currents along the zigzag direction for the B-doped BlueP sheet are larger than that of pristine BlueP, which implies the chemical adsorption of Co, NH_3, NO_2 and NO on B-doped BlueP, as shown in Fig. 14(a). The required minimum voltage bias decreases from 2 to 1.2 V after NO_2 adsorption which can be attributed to spin states appeared at the energy gap, as indicated by the transmission spectrum in Fig. 9(e). Under the voltage bias of 2.2 V, the current passing through the B-doped BlueP is 0.76 μA and decreases to 0.71 μA when the

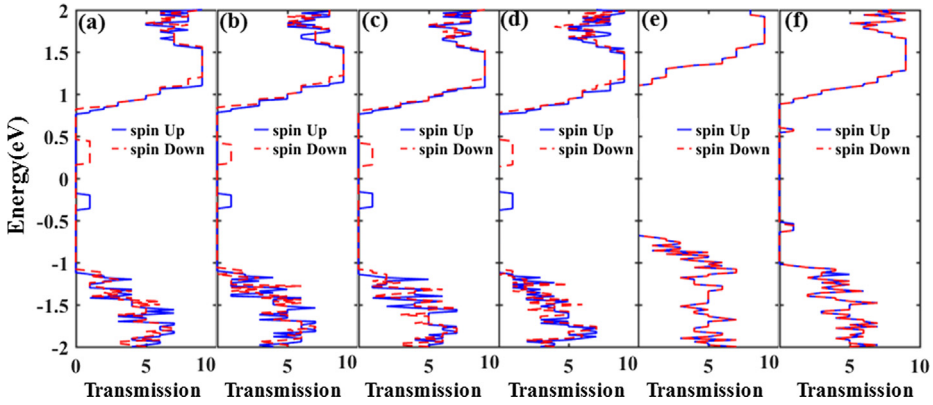

Fig. 10. The zero bias transmission spectrum of (a) C-doped BlueP before and after adsorption of the (b) CO_2, (c) CO, (d) NH_3 (e) NO_2, and (f) NO gas molecules The Fermi level is set to zero. The blue and red dashed lines represent spin up and spin down states, respectively. (For interpretation of the references to colour in this figure legend, the reader is referred to the web version of this article.)

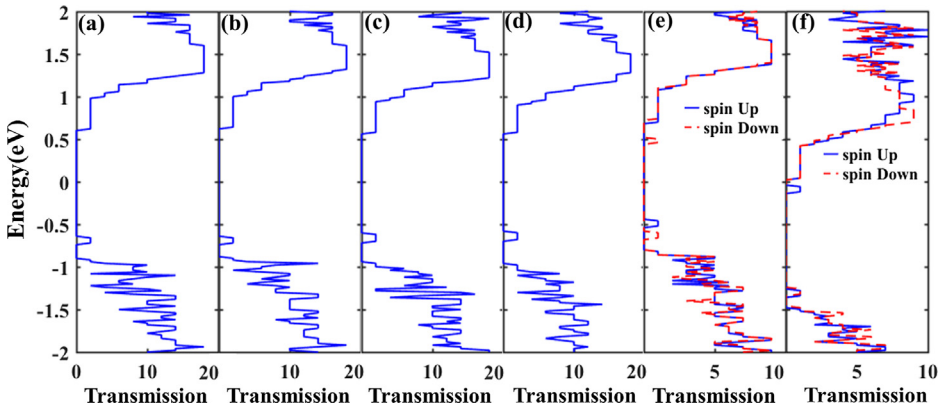

Fig. 11. The zero bias transmission spectrum of (a) N-doped BlueP before and after the adsorption of the (b) CO_2, (c) CO, (d) NH_3 (e) NO_2, and (f) NO gas molecules. The Fermi level is sel to zero. The blue and red dashed lines represent spin up and spin down states, respectively. (For interpretation of the references to colour in this figure legend, the reader is referred to the web version of this article.)

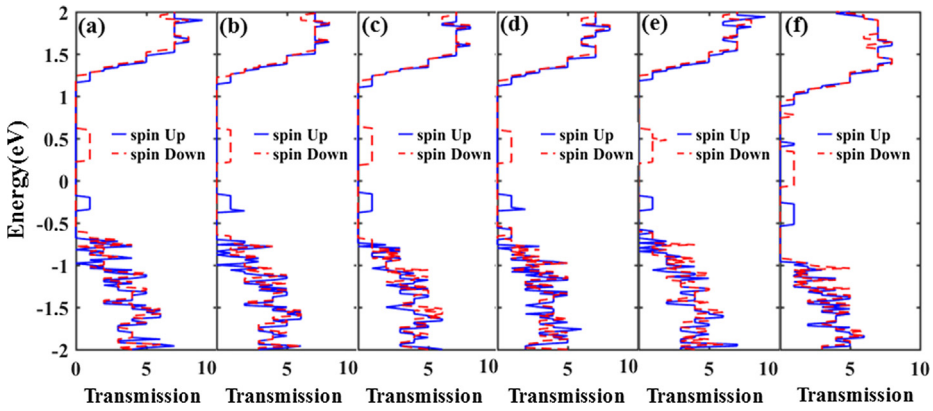

Fig. 12. The zero bias transmission spectrum of (a) O-doped BlueP before and after the adsorption of the (b) CO_2, (c) CO, (d) NH_3 (e) NO_2, and (f) NO gas molecules. The Fermi level is sel to zero. The blue and red dashed lines represent spin up and spin down states respectively. (For interpretation of the references to colour in this figure legend, the reader is referred to the web version of this article.)

substrate is exposed to CO gas molecule. By contrast, the current increases to 1.54 and 13.20 μA when NH_3 and NO_2 gas molecules are adsorbed on the B-doped BlueP, respectively. For the voltage bias larger than 2.4 V, the current increases sharply after the adsorption of NO. The current along the armchair direction is about 10 orders of magnitude smaller than that along the zigzag direction, as shown in Fig. 14(b). We observe that when the B-doped BlueP is exposed to CO and NH_3 gas molecules current reduces at a voltage bias of 2.8 V while after the NO adsorption the current increases to 2.75 μA. All currents increase rapidly for the voltage bias larger than 2.4 V. Besides, the NO_2 adsorption on the B-doped BlueP causes a negative resistance along the armchair direction in the bias range of 2.4–2.6 V.

The NH_3 adsorbent increases the current along the zigzag direction of the C-doped BlueP to 27.95 μA under the bias of 2.6 V, see Fig. 15(a). In contrast, for the NO_2 and NO adsorption, due to strong chemisorption, where covalent bonds are formed with the substrate, a current reduction of about 48% and 54% under the same bias condition is obtained, respectively. This current reduction is elucidated as an increase in the C-doped BlueP resistance, see Fig. 15(a). Along the armchair direction the current amplitude is one-third of that in zigzag direction for C-doped BlueP, as shown in Fig. 15(b). The NH_3 adsorption on the C-doped BlueP causes a negative resistance in bias range of 2.4–2.6 V. We observe extreme reduction of the current along the armchair direction for NO_2 and NO adsorption, see Fig. 15(b). Consequently, this resistance change can be measured directly in experiment.

Fig. 16(a) exhibits the I-V characteristics of zigzag N-doped BlueP before and after the gas molecule adsorption. Under a bias of 2.2 V, the current of 1.85 μA passes through the N-doped BlueP. When the N-doped BlueP is exposed to NH_3 and NO, the conductivity increases and a current of 2.46 and 3.53 μA are passed under the same bias conditions. As the current along the armchair direction for N-doped BlueP is very small, the change in the current induced by the gas absorption is negligibly small.

We have calculated the current along the zigzag and armchair

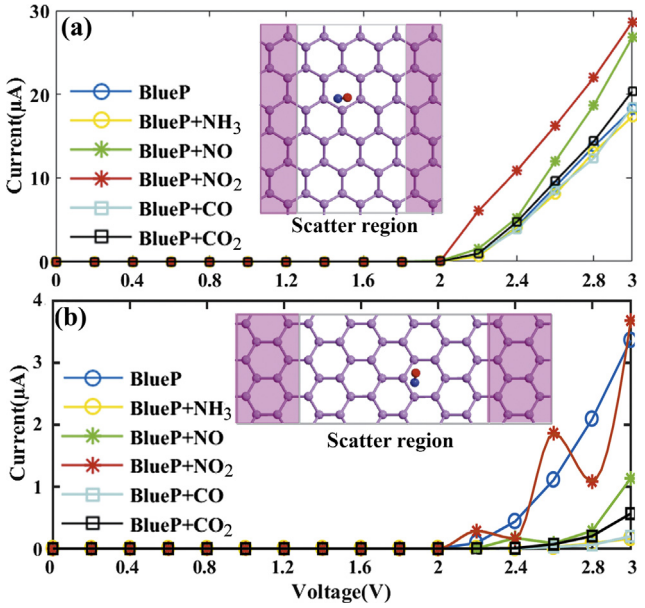

Fig. 13. I-V characteristics along the (a) zigzag and (b) armchair directions of pristine BlueP and BlueP with the gas molecules adsorption. The insets display the two-probe systems where left and right electrode regions (pink shaded region) are in contact with the central scattering region along the zigzag or armchair directions. (For interpretation of the references to colour in this figure legend, the reader is referred to the web version of this article.)

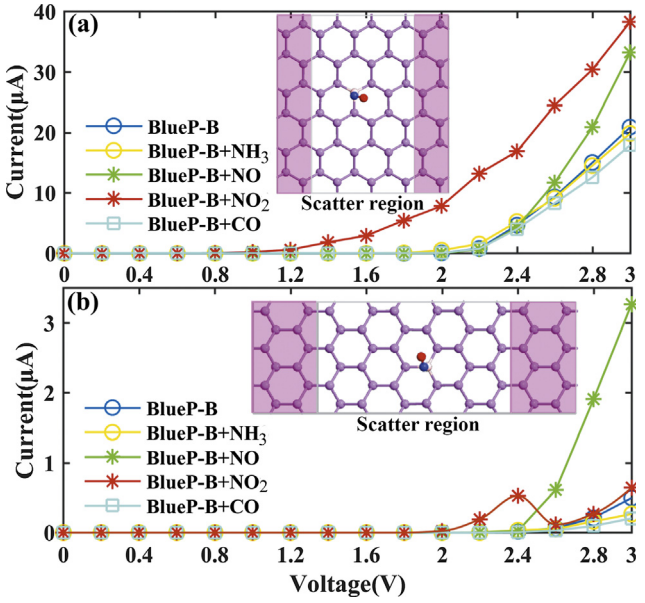

Fig. 14. I-V characteristics along the (a) zigzag and (b) armchair directions of B-doped BlueP and B-doped BlueP with the gas molecules adsorption. The insets display the two-probe systems where left and right electrode regions (pink shaded region) are in contact with the central scattering region along the zigzag or armchair directions. (For interpretation of the references to colour in this figure legend, the reader is referred to the web version of this article.)

directions for the O-doped BlueP before and after NO adsorption. Results are shown in Fig. 17(a) and (b). As depicted in Fig. 17(a), upon NO adsorption, the current along the zigzag direction is ~4 times larger than that of pristine BlueP under the bias of 3 V. The current along the armchair direction is about 10 orders of magnitude smaller than that for the zigzag direction. Under a bias of 2.6 V, the current passing through the O-doped BlueP is 1.83 μA, but the current under the same bias condition increases to 3.18 μA after the adsorption of NO gas molecule.

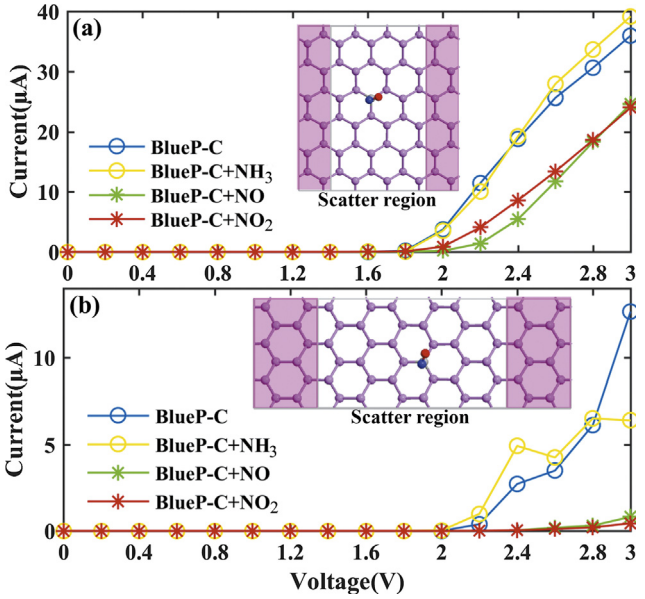

Fig. 15. I-V characteristics along the (a) zigzag and (b) armchair directions of C-doped BlueP and C-doped BlueP with the gas molecules adsorption. The insets display the two-probe systems where left and right electrode regions (pink shaded region) are in contact with the central scattering region along the zigzag or armchair directions. (For interpretation of the references to colour in this figure legend, the reader is referred to the web version of this article.)

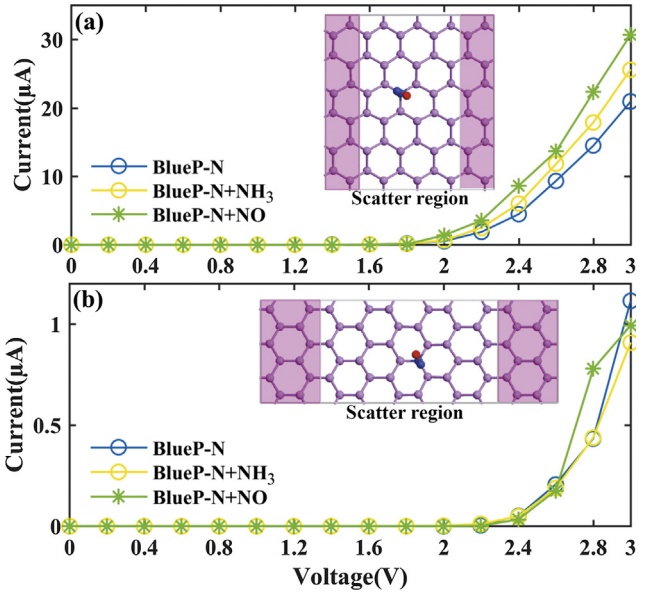

Fig. 16. I-V characteristics along the (a) zigzag and (b) armchair directions of N-doped BlueP and N-doped BlueP with the gas molecules adsorption. The insets display the two-probe systems where left and right electrode regions (pink shaded region) are in contact with the central scattering region along the zigzag or armchair directions. (For interpretation of the references to colour in this figure legend, the reader is referred to the web version of this article.)

4. Conclusion

In summary, using first-principle calculations, we have studied the structure, charge transfer, adsorption energies, electronic and transport properties of the NH_3, NO, NO_2, CO, and CO_2 adsorbed on pristine, B-, C-, N-, O- doped BlueP. The results indicate that the gas molecule adsorption on BlueP and its doped systems can either increase or decrease the current passing through it and consequently alter the resistance which can be measured directly by experiment. For B-doped and C-

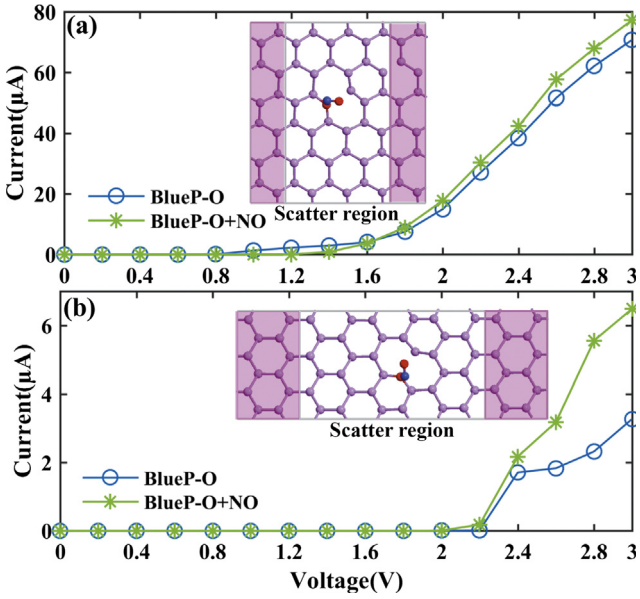

Fig. 17. I-V characteristics along the (a) zigzag and (b) armchair directions of O-doped BlueP and O-doped BlueP with the gas molecules adsorption. The insets display the two-probe systems where left and right electrode regions (pink shaded region) arc in contact with the central scattering region along the zigzag or armchair directions. (For interpretation of the references to colour in this figure legend, the reader is referred to the web version of this article.)

doped BlueP, the sensitivity to NH_3 gas molecules is improved while the sensitivity to CO gas molecules is enhanced only in B-doped BlueP. The results render BlueP and its doped systems as suitable candidates for gas detectors and future gas sensing applications.

5. Conflicts of interest

There are no conflicts of interest to declare.

Acknowledgements

This paper was partially supported by Nanoelectronic Center of Excellence, department of electrical and computer engineering, University of Tehran and Presidency of Islamic Republic of Iran National Elites Foundation.

References

[1] B. Huang, et al., Adsorption of gas molecules on graphene nanoribbons and its implication for nanoscale molecule sensor, J. Phys. Chem. C 112 (35) (2008) 13442–13446.
[2] C. Liu, C.S. Liu, X. Yan, Arsenene as a promising candidate for NO and NO_2 sensor: a first-principles study, Phys. Lett. Sect. A Gen. At. Solid State Phys. 381 (12) (2017) 1092–1096.
[3] H. Liu, et al., Phosphorene: an unexplored 2D semiconductor with a high hole mobility, ACS Nano 8 (4) (2014) 4033–4041.
[4] Y. Du, H. Liu, Y. Deng, P.D. Ye, Device perspective for black phosphorus field-effect transistors: contact resistance, ambipolar behavior, and scaling, ACS Nano 8 (10) (2014) 10035–10042.
[5] L. Li, et al., Black phosphorus field-effect transistors, Nat. Nanotechnol. 9 (5) (2014) 372–377.
[6] M. Buscema, D.J. Groenendijk, S.I. Blanter, G.A. Steele, H.S.J. Van Der Zant, A. Castellanos-Gomez, Fast and broadband photoresponse of few-layer black phosphorus field-effect transistors, Nano Lett. 14 (6) (2014) 3347–3352.
[7] J. Na, et al., Few-layer black phosphorus field-effect transistors with reduced current fluctuation, ACS Nano 8 (11) (2014) 11753–11762.
[8] F. Xia, H. Wang, Y. Jia, Rediscovering black phosphorus as an anisotropic layered material for optoelectronics and electronics, Nat. Commun. 5 (2014).
[9] J. Qiao, X. Kong, Z.X. Hu, F. Yang, W. Ji, High-mobility transport anisotropy and linear dichroism in few-layer black phosphorus, Nat. Commun. 5 (2014).
[10] J. Kim, et al., Observation of tunable band gap and anisotropic dirac semimetal state in black phosphorus, Science (80-) 349 (6249) (2015) 723–726.
[11] L. Kou, C. Chen, S.C. Smith, Phosphorene: fabrication, properties, and applications, J. Phys. Chem. Lett. 6 (14) (2015) 2794–2805.
[12] A.J. Yang, et al., Phosphorene: a promising candidate for highly sensitive and selective SF_6 decomposition gas sensors, IEEE Electron Device Lett. 38 (7) (2017) 963–966.
[13] L. Kou, T. Frauenheim, C. Chen, Phosphorene as a superior gas sensor: selective adsorption and distinct i-V response, J. Phys. Chem. Lett. 5 (15) (2014) 2675–2681.
[14] Y. Cai, Q. Ke, G. Zhang, Y.W. Zhang, Energetics, charge transfer, and magnetism of small molecules physisorbed on phosphorene, J. Phys. Chem. C 119 (6) (Feb. 2015) 3102–3110.
[15] A. Srivastava, M.S. Khan, S.K. Gupta, R. Pandey, Unique electron transport in ultrathin black phosphorene: Ab-initio study, Appl. Surf. Sci. 356 (2015) 881–887.
[16] Q. Yang, et al., First-principles study of sulfur dioxide sensor based on phosphorenes, IEEE Electron Device Lett. 37 (5) (2016) 660–662.
[17] S. Guo, L. Yuan, X. Liu, W. Zhou, X. Song, S. Zhang, First-principles study of SO_2 sensors based on phosphorene and its isoelectronic counterparts: GeS, GeSe, SnS, SnSe, Chem. Phys. Lett. 686 (2017) 83–87.
[18] V. Nagarajan, R. Chandiramouli, Adsorption of NO_2 molecules on armchair phosphorene nanosheet for nano sensor applications–a first-principles study, J. Mol. Graph. Model. 75 (2017) 365–374.
[19] Z. Zhu, D. Tománek, Semiconducting layered blue phosphorus: a computational study, Phys. Rev. Lett. 112 (17) (2014) 176802.
[20] J.L. Zhang, et al., Epitaxial growth of single layer blue phosphorus: a new phase of two-dimensional phosphorus, Nano Lett. 16 (8) (2016) 4903–4908.
[21] H.C. Luo, et al., First-principles study of nitric oxide sensor based on blue phosphorus monolayer, IEEE Electron Device Lett. 38 (8) (2017) 1139–1142.
[22] B. Salmankurt, H.H. Gürel, Modifying of gas adsorption on phosphorene (2017) 120007.
[23] N. Liu, S. Zhou, Gas adsorption on monolayer blue phosphorus: implications for environmental stability and gas sensors, Nanotechnology 28 (17) (2017) 175708.
[24] J.M. Soler, et al., The SIESTA method for ab initio order- N materials simulation, J. Phys. Condens. Matter 14 (11) (Mar. 2002) 2745–2779.
[25] J.P. Perdew, K. Burke, M. Ernzerhof, Generalized gradient approximation made simple, Phys. Rev. Lett. 77 (18) (1996) 3865–3868.
[26] S. Grimme, Semiempirical GGA-type density functional constructed with a long-range dispersion correction, J. Comput. Chem. 27 (15) (2006) 1787–1799.
[27] M. Brandbyge, J.L. Mozos, P. Ordejón, J. Taylor, K. Stokbro, Density-functional method for nonequilibrium electron transport, Phys. Rev. B - Condens. Matter Mater. Phys. 65 (16) (2002) 1654011–16540117.
[28] M. Topsakal, V.M.K. Bagci, S. Ciraci, Current-voltage (I-V) characteristics of armchair graphene nanoribbons under uniaxial strain, Phys. Rev. B 81 (20) (2010) 205437.
[29] M. Sun, W. Tang, Q. Ren, S.K. Wang, J. Yu, Y. Du, A first-principles study of light non-metallic atom substituted blue phosphorene, Appl. Surf. Sci. 356 (2015) 110–114.
[30] H. Zheng, H. Yang, H. Wang, X. Du, Y. Yan, Electronic and magnetic properties of nonmetal atoms doped blue phosphorene: first-principles study, J. Magn. Magn. Mater. 408 (2016) 121–126.
[31] X.-B. Li, P. Guo, T.-F. Cao, H. Liu, W.-M. Lau, L.-M. Liu, Structures, stabilities and electronic properties of defects in monolayer black phosphorus, Sci. Rep. 5 (1) (2015) 10848.
[32] P. Pyykkö, M. Atsumi, Molecular single-bond covalent radii for elements 1–118, Chem. - A Eur. J. 15 (1) (Jan. 2009) 186–197.
[33] X. Peng, Q. Wei, A. Copple, Strain-engineered direct-indirect band gap transition and its mechanism in two-dimensional phosphorene, Phys. Rev. B 90 (8) (2014) 085402.